

## Point-to-point responses

*We appreciate the reviewers for their valuable and constructive comments, which are very helpful for the improvement of the manuscript. We have revised the manuscript carefully according to the reviewers' comments. We have addressed the reviewers' comments on a point-to-point basis as below for consideration, where the reviewers' comments are cited in **black**, and the responses are in **blue**.*

### Editor

1) A "Short summary" system section contains scientific abbreviations. Please note, if you used scientific abbreviations without giving the written-out explanation, these must be written out with the next file upload request. However, do not forget that there is a limit to characters (not words!) for "Short summary": it must be < 500 characters.

Re: Thanks for your great comment. We have deleted some unnecessary details and reorganized the languages as below:

“Vertical profile observations are key to understanding regional air pollution but remain scarce due to existing limits. This study presents a high-time-resolution (~15 minutes) dataset of aerosol, nitrogen dioxide and formaldehyde vertical profiles from 32 sites in China (2019–2023) using passive remote sensing. It documents vertical distribution, seasonal variations and diurnal pattern, revealing long-term trends. Available at Zenodo: <https://doi.org/10.5281/zenodo.14194965>; Jiao et al., 2024.”

2) Figure 1 may contain a territory that is disputed according to the United Nations. If and when the manuscript is accepted for final revised publication, you will be asked to choose one of the following options: (a) you could remove the disputed territory from the map and submit new figure files, or (b) we could add a statement that some figures contain disputed territories.

Re: Thank you for your careful consideration of our manuscript. We fully recognize the sensitivity surrounding the disputed territories and are committed to addressing this issue appropriately. After a comprehensive evaluation and careful consideration, we have decided to remove Figure 1 from the revised manuscript. Importantly, the site distribution information originally presented in Figure 1 can be fully and accurately conveyed through other sections of the manuscript. Specifically, Table 1 provides a detailed list of the regional distribution and geographic coordinates of each monitoring site, while Table S1 offers information on site type (e.g., urban, suburban, rural) and major emission sources in the surrounding areas, ensuring the scientific rigor and integrity of the manuscript. We hope this approach adequately addresses concerns related to the disputed territories. Once again, we sincerely appreciate your valuable comments and guidance.

### Referee #1

Jiao et al. present a comprehensive dataset of vertical profile observations of aerosol, NO<sub>2</sub>, and HCHO in China from 2019 to 2023 using a hyperspectral remote sensing network. The dataset fills a critical gap in vertical profile monitoring, providing high temporal resolution and wide geographic coverage. The manuscript is well-organized and offers valuable insights into the spatial-temporal variations of atmospheric components, which can inform environmental policies and enhance scientific modeling. However, there are several areas where the manuscript could be improved to enhance clarity, accuracy, and impact.

1) Section 2.2 mentions data filtering criteria (e.g., DOF, relative error thresholds), but the rationale behind these criteria needs to be explained in more detail. In addition, it is recommended to include a

specific site example to demonstrate the differences in data distribution before and after filtering.

Re: Thanks for your great comments. In response to the comment regarding the explanation of the data filtering criteria, we have added Section S1 in the supplement, where we provide a detailed description of this process. Additionally, we have selected the CAMS and HNI sites as examples and included Table S3 in the supplement, which demonstrates the differences in the data before and after the application of the data filtering procedures. The content of Section S1 is as follows:

“Section S1. Data Filtering Criteria and Principles

**DOF (Degrees of Freedom):** In the retrieval process, the averaging kernel matrix reflects the sensitivity of the observation data to the state vector transformation. The sum of the diagonal elements of this matrix represents the Degrees of Freedom (DOF), which quantifies the amount of independent information that can be effectively extracted from the observational data. A higher DOF indicates that more independent information has been extracted, whereas a lower DOF suggests that the observation data is not sensitive to changes in the state vector. Consequently, we exclude data with a DOF value lower than 1.0, as this typically indicates that the retrieval process has not effectively utilized the observational data, leading to potentially unreliable results or higher uncertainty.

**$\chi^2$  (Chi-Square):** As shown in Equation (1), the  $\chi^2$  value is used to assess the model fit, i.e., the difference between the model predictions and the actual observed values. A smaller  $\chi^2$  value indicates that the model closely matches the observed values, while a larger  $\chi^2$  value suggests a significant discrepancy, which may arise from inaccurate prior information, systematic errors, or other unaccounted factors. In order to ensure the quality and reliability of the analysis, we exclude data with  $\chi^2$  values greater than 200. This threshold helps to minimize the influence of outliers and ensures that the results are based on high-quality data.

$$\chi^2 = (\mathbf{y} - F(\mathbf{x}, \mathbf{b}))^T \mathbf{S}_\epsilon^{-1} (\mathbf{y} - F(\mathbf{x}, \mathbf{b})) + (\mathbf{x} - \mathbf{x}_a)^T \mathbf{S}_a^{-1} (\mathbf{x} - \mathbf{x}_a) , \quad (1)$$

**SZA (Solar Zenith Angle):** In this study, we focus on the absorption in the troposphere near the Earth’s surface. When the solar zenith angle (SZA) exceeds 75°, the predominant scattering transpire within the lower stratosphere and upper troposphere (Song et al., 2023).

In this case, DOAS measurements exhibit heightened sensitivity towards stratospheric absorption, while demonstrating reduced sensitivity to absorption in the proximity of the surface. Therefore, measurements with SZA > 75° are excluded from the analysis.

**CI (Color Index):** The color index (CI) is defined as the ratio of the spectral intensities at 330 nm and 390 nm, and is used to identify potential cloud interference (Wagner et al., 2016). A polynomial function of time is fitted to the data from clear days without significant cloud cover to establish the diurnal CI variation pattern. Based on this fitted model, a CI threshold is determined for each time point. If the CI value at a given time is below 10% of the threshold, it is assumed that the data are affected by cloud interference, and such data are excluded from further analysis (Ryan et al., 2018).

**Relative Retrieval Error:** The relative retrieval error measures the precision of the retrieval results. If the relative error exceeds 50%, the result is considered to have too high an uncertainty and is therefore excluded as unreliable data (Tan et al., 2018).

Due to the peculiarity of the instrument’s data collection and storage process, data with SZA and CI values that do not meet the criteria are excluded prior to processing. After filtering based on DOF,  $\chi^2$ , and relative retrieval error, approximately 10% of the data is discarded.”

The content of Table S3 is as follows:

“Table S3. Differences in the data before and after filtering based on DOF,  $\chi^2$ , and relative retrieval error, using the CAMS and HNI stations as examples. The numbers in the table represent the monthly data integrity at each site, indicating the ratio of days with and without data in a month.”

	CAMS	CAMS (filtered)	HNI	HNI (filtered)
--	------	-----------------	-----	----------------

2019-01	1.00	1.00	0.00	0.00
2019-02	1.00	1.00	0.00	0.00
2019-03	0.94	0.94	0.00	0.00
2019-04	0.67	0.67	0.07	0.07
2019-05	0.87	0.87	0.06	0.06
2019-06	0.97	0.97	0.97	0.97
2019-07	1.00	1.00	1.00	0.97
2019-08	0.42	0.42	0.48	0.48
2019-09	0.43	0.43	0.00	0.00
2019-10	0.94	0.94	0.00	0.00
2019-11	1.00	1.00	0.97	0.97
2019-12	0.68	0.68	0.94	0.94
2020-01	0.94	0.94	1.00	1.00
2020-02	0.97	0.97	1.00	1.00
2020-03	1.00	1.00	1.00	1.00
2020-04	1.00	1.00	0.93	0.93
2020-05	1.00	1.00	0.94	0.94
2020-06	1.00	1.00	1.00	0.97
2020-07	1.00	1.00	0.39	0.39
2020-08	1.00	1.00	0.00	0.00
2020-09	0.97	0.97	0.00	0.00
2020-10	0.97	0.97	0.00	0.00
2020-11	0.83	0.83	0.93	0.90
2020-12	0.97	0.97	1.00	1.00
2021-01	0.97	0.97	0.94	0.94
2021-02	0.93	0.93	0.79	0.79
2021-03	0.00	0.00	0.52	0.52
2021-04	0.27	0.27	0.27	0.27
2021-05	0.97	0.97	0.77	0.77
2021-06	0.97	0.97	0.80	0.80
2021-07	0.48	0.48	0.84	0.84
2021-08	0.00	0.00	0.81	0.81
2021-09	0.00	0.00	0.43	0.43
2021-10	0.65	0.65	0.16	0.16
2021-11	0.77	0.77	0.67	0.67
2021-12	1.00	1.00	1.00	1.00
2022-01	0.97	0.97	0.81	0.81
2022-02	1.00	1.00	0.96	0.96
2022-03	1.00	1.00	1.00	1.00
2022-04	0.20	0.20	0.67	0.67
2022-05	0.55	0.55	0.00	0.00
2022-06	1.00	1.00	0.00	0.00
2022-07	1.00	1.00	0.00	0.00
2022-08	1.00	1.00	0.00	0.00
2022-09	1.00	1.00	0.00	0.00
2022-10	1.00	1.00	0.00	0.00

2022-11	0.97	0.97	0.00	0.00
2022-12	0.45	0.45	0.00	0.00
2023-01	1.00	0.97	0.00	0.00
2023-02	0.57	0.57	0.00	0.00
2023-03	1.00	1.00	0.00	0.00
2023-04	0.87	0.87	0.00	0.00
2023-05	0.90	0.90	0.00	0.00
2023-06	0.97	0.97	0.00	0.00
2023-07	0.97	0.97	0.00	0.00
2023-08	0.90	0.90	0.00	0.00
2023-09	0.77	0.77	0.00	0.00
2023-10	0.29	0.29	0.00	0.00

2) In Section 3.4 (Validation), the manuscript shows good correlations between the dataset and CNEMC and TROPOMI data. However, there is a lack of a detailed discussion on the potential biases and uncertainties in these comparisons. For example, how do the differences in spatial and temporal resolution between MAX-DOAS and TROPOMI contribute to the observed discrepancies?

Re: Thank you for your insightful comment. We agree that it is essential to illustrate the potential biases and uncertainties in the comparison between our dataset and the TROPOMI and CNEMC data. To provide a more comprehensive explanation, we discuss the sources of these potential discrepancies as follows:

Firstly, MAX-DOAS typically provides high-resolution, site-specific measurements, whereas TROPOMI offers averaged values over larger spatial grids. This difference in spatial resolution can introduce discrepancies when comparing data from the same geographic area. For instance, localized pollution hotspots detected by MAX-DOAS may be averaged out in TROPOMI data, potentially leading to a dilution of the observed concentrations. However, the comparison between these datasets remains valid, as both capture important atmospheric features, albeit with different spatial representativeness. The robust correlation observed between these datasets suggests that, despite the spatial differences, the overall trends and patterns of atmospheric composition are well captured.

Additionally, although MAX-DOAS data were averaged over a 30-minute window to align with TROPOMI's overpass time, there may still be potential discrepancies caused by instantaneous variations in meteorological conditions and pollution sources. For example, rapid weather changes or localized pollution events could cause significant concentration fluctuations that are more pronounced on shorter timescales, leading to discrepancies between the datasets. Nevertheless, despite these potential short-term deviations, the broad atmospheric trends are accurately represented.

Furthermore, the CNEMC data has a higher temporal resolution and typically aligns well with the MAX-DOAS measurements. However, there are differences in both location and distance between the CNEMC stations and the MAX-DOAS sites, which may introduce some discrepancies. This discrepancy is especially evident in regions with heterogeneous pollution sources. To illustrate this potential difference, we calculated the distance between each MAX-DOAS site and the nearest CNEMC station, as shown in Table S4. The strong correlation between the MAX-DOAS and CNEMC data further supports the reliability of our dataset.

In parallel, it is important to note that the MAX-DOAS sites measure the path-integrated average concentration along the observation line of sight, while the CNEMC stations focus on point-specific concentration measurements at fixed locations, providing highly localized concentration data. Although the two methods differ in data acquisition, our dataset has undergone rigorous quality control and calibration procedures to ensure its accuracy and reliability. It provides valuable insights into the broader distribution of pollutants, demonstrating its effectiveness and credibility in air quality monitoring.

Finally, it is important to note that despite these inherent uncertainties, our data and the related validation demonstrate strong credibility and provide a reliable foundation for the conclusions drawn.

3) While the dataset covers seven major regions, monitoring sites are fewer in regions such as Central and Southwest China. The manuscript should discuss how this uneven distribution might impact regional representativeness and the generalizability of the results.

Re: Thank you for your valuable comments. Regarding the potential impact of uneven site distribution on regional representativeness and the generalizability of the results, while our dataset covers seven major geographical regions of China and provides valuable information on atmospheric composition across the country, we acknowledge that the number of monitoring sites is relatively limited in regions such as Central China and Southwest China (1 and 2 stations, respectively), while the North and East regions have a higher density of stations (9 and 13 stations, respectively). This uneven distribution could indeed affect the regional representativeness and the general applicability of the results. Specifically, the regions with fewer sites may not fully capture the spatial and temporal variations in atmospheric composition, especially considering the complex and diverse topography of these areas (e.g., mountains, basins, and plains). A limited number of sites may struggle to capture all the significant environmental features and pollution dynamics within these regions. For instance, the mountainous and canyon terrain in the Southwest may lead to different pollutant dispersion and accumulation patterns compared to the plains. As a result, we have revised the summary to include a discussion on the limitations of the dataset. The revised section is as follows:

Line 384, “(4) In regions such as Central China and Southwest China, the number of monitoring sites is relatively limited. This uneven distribution may potentially affect the representativeness of the results for these areas.”

Although there are certain limitations, we are confident in the overall quality of the dataset presented in the manuscript. First, the dataset provides atmospheric composition observation data across the entire country, encompassing a variety of geographical environments, from urban centers to remote mountainous areas, offering a wealth of valuable information. Second, the high-resolution observations at each station capture subtle variations in local atmospheric composition, which is crucial for understanding inter-regional differences. Additionally, the reliability and accuracy of the data have been further strengthened through comparison with ground-based data from CNEMC and satellite data from TROPOMI.

Future work will focus on expanding the network of monitoring sites, with particular emphasis on increasing the station density in Central China, Southwest China, Northeast China, and Northwest China. This expansion aims to ensure the comprehensiveness and representativeness of the dataset, addressing the current uneven distribution and enhancing the overall coverage of the monitoring network.

4) Technical comments.

Line 26.

‘Its sharing would facilitate the scientific community in exploring of source-receptor relationships’ -> ‘Its sharing would facilitate the scientific community in exploring source-receptor relationships’.

Re: Thanks for your comment. You are correct that the sentence does indeed contain the issue you mentioned. When we shortened the abstract to meet the required word limit, we removed the problematic sentence.

Line 42.

‘Aerosol, as one of the most complex and critical composition of the atmospheric environment’ -> ‘Aerosol, as one of the most complex and critical compositions of the atmospheric environment’.

Re: Thanks for your comment. We have rewritten this sentence as “Aerosol, as one of the most complex

and critical compositions of the atmospheric environment”.

Line 98.

‘It helps provide a complete perspective on the vertical distribution of aerosol, NO<sub>2</sub>, and HCHO in China’ -> ‘The diversity of these monitoring sites helps provide a complete perspective on the vertical distribution of aerosol, NO<sub>2</sub>, and HCHO in China’.

Re: Thanks for your comment. We have rewritten this sentence as “The diversity of these monitoring sites helps provide a complete perspective on the vertical distribution of aerosol, NO<sub>2</sub>, and HCHO in China”.

Line 108.

‘...which located in China’s economically developed and densely populated areas’ -> ‘...which are located in China’s economically developed and densely populated areas’.

Re: Thanks for your comment. We have rewritten this sentence as “...which are located in China’s economically developed and densely populated areas”.

Line 110.

‘offer vertical distribution data across different elevation’ -> ‘offer vertical distribution data across different elevations’.

Re: Thanks for your comment. We have rewritten this sentence as “Sites at Mount Tai (TS) and Taian (TA), located at 1500 and 170 m respectively, offer vertical distribution data across different elevations”.

Line 223.

‘AECs in spring, summer, autumn, and winter accounts for 23.60%, 24.63%, 24.69%, and 27.08% of the total averaged values of four seasons, respectively’ -> ‘AECs in spring, summer, autumn, and winter account for 23.60%, 24.63%, 24.69%, and 27.08% of the total averaged values of four seasons, respectively’.

Re: Thanks for your comment. We have rewritten this sentence as “AECs in spring, summer, autumn, and winter account for 23.60%, 24.63%, 24.69%, and 27.08% of the total averaged values of four seasons, respectively”.

Line 237.

‘High-concentration aerosol with extinction coefficients exceeding 1.0 km<sup>-1</sup> are primarily distributed below 600 m, while aerosol with extinction coefficients greater than 0.6 km<sup>-1</sup> are concentrated below 1000 m’ -> ‘High-concentration aerosols with extinction coefficients exceeding 1.0 km<sup>-1</sup> are primarily distributed below 600 m, while aerosols with extinction coefficients greater than 0.6 km<sup>-1</sup> are concentrated below 1000 m’.

Re: Thanks for your comment. We have rewritten this sentence as “High-concentration aerosols with extinction coefficients exceeding 1.0 km<sup>-1</sup> are primarily distributed below 600 m, while aerosols with extinction coefficients greater than 0.6 km<sup>-1</sup> are concentrated below 1000 m”.

Line 240.

‘with one peak occurring before 12:00 BJT and the other between 16:00 and 18:00 BJT’ -> ‘with one peak occurring before 12:00 Beijing Time (BJT) and the other between 16:00 and 18:00 BJT’.

Re: Thanks for your comment. We have rewritten this sentence as “At many sites, the AEC exhibits a bimodal pattern, with one peak occurring before 12:00 Beijing Time (BJT) and the other between 16:00 and 18:00 BJT”.

Line 243.

‘located in the central Beijing’ -> ‘located in central Beijing’.

Re: Thanks for your comment. We have rewritten this sentence as “This bimodal pattern is more pronounced at urban sites such as CAMS, IAP (located in central Beijing) and SH\_XH (located in central Shanghai), likely due to the significant contribution of traffic emissions during morning and evening rush hours.”.

Line 287.

‘The averaged near-surface NO<sub>2</sub> concentrations in spring, summer, autumn, and winter accounts for 23.06%, 16.57%, 25.74%, and 34.63% of the total averaged values of four seasons, respectively’ -> ‘The averaged near-surface NO<sub>2</sub> concentrations in spring, summer, autumn, and winter account for 23.06%, 16.57%, 25.74%, and 34.63% of the total averaged values of four seasons, respectively’.

Re: Thanks for your comment. We have rewritten this sentence as “The averaged near-surface NO<sub>2</sub> concentrations in spring, summer, autumn, and winter account for 23.06%, 16.57%, 25.74%, and 34.63% of the total averaged values of four seasons, respectively”.

Line 310.

‘transportation’ -> ‘transportation from’.

Re: Thanks for your comment. We have rewritten this sentence as “HCHO originates from diverse sources, including fossil fuel combustion (Ho et al., 2012; Schauer et al., 2002), biomass burning (Carlier et al., 1986; Lee et al., 1997), transportation from, and industrial activities (Buzcu Guven and Olaguer, 2011)”.

## Referee #2

This manuscript presents a high-time resolution dataset of vertical profile of aerosol, NO<sub>2</sub> and HCHO across 32 sites in seven major regions of China from 2019 to 2023, which obtained from the hyperspectral vertical remote sensing network in China. It provides a comprehensive analysis of the patterns of the vertical distribution, seasonal variations and diurnal pattern of these pollutants, and comparisons with the CNEMC stations and the TROPOMI satellite data were conducted and the quality of the present dataset was analyzed. This work is quite challenging, not only because of the complexity of the observation environment, for example, the observation sites include both the Tibetan Plateau and the coastal zone; at the same time, the stability and reliability of the MAX-DOAS work in different observation environments also bring challenges to the data retrievals. Whatever, the good agreement with TROPOMI satellite and ground-based CNEMC measurements showed the data quality is assured.

The dataset it provides could be useful for future scholars in the fields of atmosphere environment and climate change. Overall, this is a good paper that deserves to be published in ESSD. Nevertheless, some minor issues must be clarified.

1) First, the information about the 32 sites is limited, more description should be provided, including the major emission sources around the each site and the site type (urban, suburban, background etc.) and observation period in each site suggested to be added in Table 1. It is important to understand the seasonal and diurnal pattern of the observed pollutants.

Re: Thank you for your valuable comment. We agree that further description and additional details of the sites are necessary. To improve readability, we have included Table S2 in supplement to describe the observation periods for each site. Additionally, Table S1 in supplement provides information on the main emission sources surrounding each site, as well as the site types. We hope these additions will offer a more comprehensive and accessible overview for the readers.

Table S1. The site type and the major emission sources around each site.

No.	Region	Site(code)	Site Type	Major emission sources
1	North China	Chinese Academy of Meteorological Sciences (CAMS)	Urban	Traffic emissions, residential heating, industrial activities
2		The Institute of Atmospheric Physics (IAP)	Urban	Traffic emissions, residential heating, industrial activities
3		Nancheng (NC)	Suburban	Agricultural activities, light industrial emissions
4		University of Chinese Academy of	Suburban	Traffic emissions, residential heating

		Sciences (UCAS)		
5		Wangdu (WD)	Rural	Agricultural activities, biomass burning
6		Xianghe (XH)	Rural	Agricultural activities, biomass burning
7		Shijiazhuang (SJZ)	Urban	Heavy industrial emissions, traffic emissions, residential heating
8		Shanxi University (SXU)	Urban	Industrial emissions, traffic emissions
9		Inner Mongolia Normal University (IMNU)	High-altitude	Dust emissions, agricultural activities
10	East China	Dongying (DY)	Coastal	Oil refineries, petrochemical industries, traffic emissions
11		Qingdao (QD)	Coastal	Ship emissions, industrial activities, traffic emissions
12		Taishan (TS)	High-altitude	Background site, minimal local emissions
13		Tai'an(TA)	Urban	Traffic emissions, industrial activities
14		Shanghai_Xuhui (SH_XH)	Urban	Heavy traffic emissions, industrial activities, residential heating
15		Shanghai_Dianshan Lake (SH_DL)	Lakeside	Traffic emissions, industrial activities, ship emissions
16		Nanjing University of Information Science and Technology (NUIST)	Coastal	Traffic emissions, industrial activities, ship emissions
17		Ningbo (NB)	Coastal	Ship emissions, industrial activities, traffic emissions
18		Huaniao Island (HNI)	Coastal	Ship emissions, minimal local emissions
19		Lin'an(LA)	Rural	Agricultural activities, biomass burning
20		Huaibei Normal University (HNU)	Urban	Industrial emissions, traffic emissions
21		Anhui University (AHU)	Urban	Traffic emissions, industrial activities
22		Changfeng(CF)	Suburban	Traffic emissions, agricultural activities
23	South China	Xiamen_Institute of Urban Environment (IUE)	Urban	Traffic emissions, industrial activities, ship emissions
24		Guangzhou Institute of Geochemistry (GIG)	Urban	Traffic emissions, industrial activities, ship emissions
25		Southern University of Science and Technology (SUST)	Urban	Traffic emissions, industrial activities
26	Southwest China	Shangri-La Station (SLS)	High-altitude	Background site, minimal local emissions
27		Chongqing (CQ)	Urban	Heavy industrial emissions, traffic emissions
28	Northwest China	Lanzhou University (LZU)	Urban	Industrial emissions, traffic emissions, dust storms
29		Xi'an (XA)	Urban	Traffic emissions, industrial activities
30	Northeast	Juehua Island (JHI)	Coastal	Ship emissions, minimal local emissions

	China			
31		Liaoning University (LNU)	Urban	Industrial emissions, traffic emissions
32	Central China	Luoyang (LY)	Urban	Heavy industrial emissions, traffic emissions

Table S2. The site observation period. The months listed in the observation period indicate that the site has data for a certain month. The specific monthly data integrity is shown in Figure 2.

No.	Region	Site(code)	Observation period	No.	Region	Site(code)	Observation period
1	North China	Chinese Academy of Meteorological Sciences (CAMS)	2019.01-2021.02 2021.04-2021.07 2021.10-2023.10 2021.04-2021.07	17	East China	Ningbo (NB)	2019.11-2020.01 2020.05-2020.06 2020.08-2021.03 2021.05-2021.06 2021.09-2021.09 2021.12-2021.12
2		The Institute of Atmospheric Physics (IAP)	2019.09-2021.03 2021.05-2021.05	18		Huaniao Island (HNI)	2019.04-2019.08 2019.11-2020.07 2020.11-2022.04
3		Nancheng (NC)	2019.01-2020.01 2020.05-2021.03 2021.07-2021.10 2021.12-2022.05	19		Lin'an(LA)	2020.12-2020.12 2021.02-2022.07
4		University of Chinese Academy of Sciences (UCAS)	2019.01-2020.02 2020.06-2021.07 2021.11-2022.07 2022.09-2023.05	20		Huaibei Normal University (HNU)	2020.06-2022.05
5		Wangdu (WD)	2019.03-2023.03 2023.06-2023.12	21		Anhui University (AHU)	2020.12-2023.09
6		Xianghe (XH)	2019.01-2019.01 2019.03-2019.10 2020.01-2021.05 2021.08-2022.01 2022.05-2022.05	22		Changfeng(CF)	2022.05-2022.12 2023.03-2023.12
7		Shijiazhuang (SJZ)	2019.10-2021.03 2021.05-2022.05	23	South China	Xiamen_Institute of Urban Environment (IUE)	2020.01-2020.03 2020.06-2020.09 2021.04-2021.05
8		Shanxi University (SXU)	2020.10-2020.11 2021.04-2022.03 2022.07-2023.07 2023.09-2023.12	24		Guangzhou Institute of Geochemistry (GIG)	2019.09-2021.10 2022.03-2023.11
9		Inner Mongolia Normal University (IMNU)	2020.07-2021.10 2022.01-2022.08 2023.10-2023.10	25		Southern University of Science and Technology (SUST)	2019.01-2021.11 2022.01-2022.12
10	East China	Dongying (DY)	2019.09-2019.09 2019.11-2020.05 2020.10-2021.07	26	Southw est China	Shangri-La Station (SLS)	2019.11-2022.08
11		Qingdao (QD)	2019.12-2020.12	27		Chongqing (CQ)	2019.01-2020.03 2020.05-2023.01 2023.03-2023.04
12		Taishan (TS)	2020.01-2020.02 2020.04-2022.07 2023.03-2023.03	28	Northw est China	Lanzhou University (LZU)	2019.01-2021.11
13		Tai'an(TA)	2021.06-2021.06 2021.08-2021.08 2021.12-2022.01	29		Xi'an (XA)	2020.01-2020.06 2020.08-2020.08
14		Shanghai_Xuhui (SH_XH)	2019.09-2020.01 2020.03-2020.12	30	Northe ast China	Juehua Island (JHI)	2020.09-2021.06
15		Shanghai_Dianshan Lake (SH_DL)	2019.01-2019.06	31		Liaoning University (LNU)	2019.07-2019.07 2019.09-2019.12
16		Nanjing University of Information Science and Technology	2019.01-2019.07 2019.09-2019.11 2022.04-2023.12	32	Central China	Luoyang (LY)	2020.02-2022.02

2) Second, as the vertical dataset covers the period of 2019-2023, which significant improvements in air quality and decrease of air pollutants at ground had been reported, it would be interesting to provide the analysis of temporal changes of the observed pollutants (aerosol, NO<sub>2</sub> and HCHO) in the upper atmosphere.

Re: Thanks for your great comments. In response to your suggestion, we have conducted a more detailed analysis of the temporal changes of pollutants (aerosols, NO<sub>2</sub>, and HCHO) observed in the upper atmosphere between 2019 and 2023 and provide a comprehensive response below:

Existing studies indicate that the most severe air pollution in China occurred approximately between 2013 and 2015 (Zheng et al., 2018), followed by significant improvements in air quality since 2017 (Ma et al., 2019). Consequently, while air quality continued to improve during the 2019–2023 period, the rate of improvement may have slowed, entering a plateau phase. This relative stability of pollutant concentrations at the surface level could also contribute to relatively modest changes in pollutant levels in the upper atmosphere.

Against this backdrop, we conducted a time series analysis of aerosol, NO<sub>2</sub>, and HCHO concentrations at various sites across different altitude layers from 2019 to 2023. As described in the manuscript, we used the 0-100m, 500-600m, and 900-1000m layers to represent the lower, middle, and upper boundary layers, respectively. The results indicate that the overall trends of the three pollutants in the upper atmosphere are generally consistent with those in the middle and lower layers. However, at certain sites and during specific periods, the trends in the lower layers may deviate from those in the middle and upper layers. Notably, interannual variations in pollutant concentrations are less pronounced in the upper atmosphere, whereas seasonal variations and diurnal patterns are more evident. Furthermore, the concentration fluctuations in the lower layers of the three pollutants are significantly greater than those in the middle and upper layers, and their concentration levels differ notably from those in the upper layers, with the most noticeable differences observed in the NO<sub>2</sub> time series. To quantify these differences, we calculated the ratios of average concentrations between altitude layers. For aerosols, the ratio of aerosol extinction coefficient in the upper layer to that in the lower layer is 33.09%, while the ratio in the middle layer to the lower layer is 64.36%. For NO<sub>2</sub>, these values are 15.29% and 32.98%, respectively, while for HCHO, the corresponding ratios are 56.36% and 80.88%. Among the three pollutants, HCHO exhibits the smallest vertical gradient, indicating that its concentration differences and fluctuations across the lower, middle, and upper layers are relatively minimal. This suggests a more uniform vertical distribution of HCHO compared to aerosols and NO<sub>2</sub>.

We have plotted the time series in Figures S1-S3 and added the relevant explanatory content in line 172 and Section S2, as follows:

Line 172, “The time series of aerosol extinction coefficient, NO<sub>2</sub> concentration, and HCHO concentration for the three altitude layers during 2019 – 2023 are shown in Figures S1-S3, with the corresponding correlation analysis provided in Section S2.”

Section S2, “Figures S1 – S3 display the time series of aerosol extinction coefficient, NO<sub>2</sub> concentration, and HCHO concentration in the lower, middle, and upper layers between 2019 and 2023. The results indicate that the overall trends of the three pollutants in the upper atmosphere are generally consistent with those in the middle and lower layers. However, at certain sites and during specific periods, the trends in the lower layers may deviate from those in the middle and upper layers. Notably, interannual variations in pollutant concentrations are less pronounced in the upper atmosphere, whereas seasonal variations and diurnal patterns are more evident. Furthermore, the concentration fluctuations in the lower layers of the three pollutants are significantly greater than those in the middle and upper layers, and their concentration levels differ notably from those in the upper layers, with the most noticeable differences observed in the NO<sub>2</sub> time series. To quantify these differences, we calculated the ratios of average concentrations between

altitude layers. For aerosols, the ratio of aerosol extinction coefficient in the upper layer to that in the lower layer is 33.09%, while the ratio in the middle layer to the lower layer is 64.36%. For NO<sub>2</sub>, these values are 15.29% and 32.98%, respectively, while for HCHO, the corresponding ratios are 56.36% and 80.88%. Among the three pollutants, HCHO exhibits the smallest vertical gradient, indicating that its concentration differences and fluctuations across the lower, middle, and upper layers are relatively minimal. This suggests a more uniform vertical distribution of HCHO compared to aerosols and NO<sub>2</sub>.”

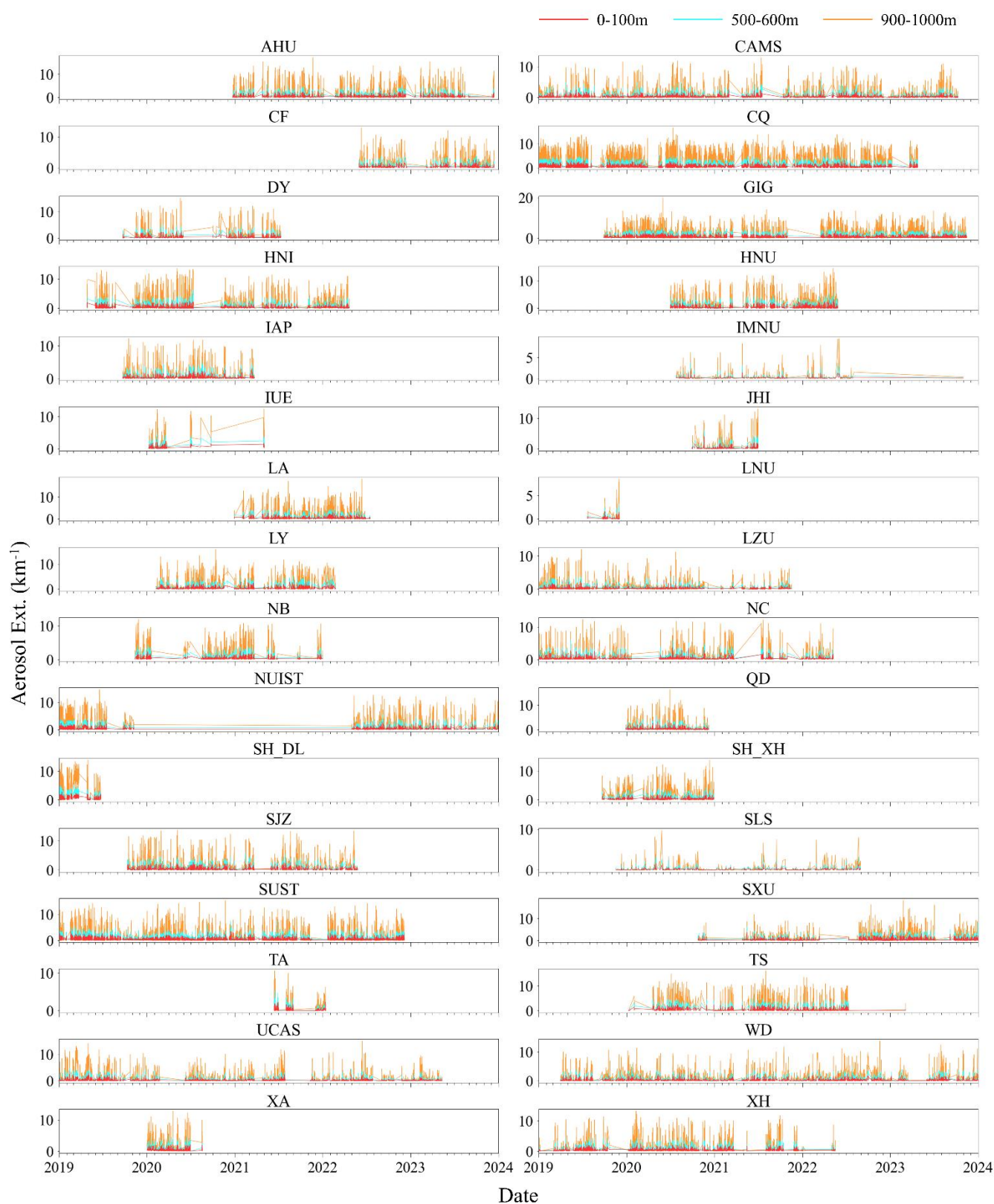
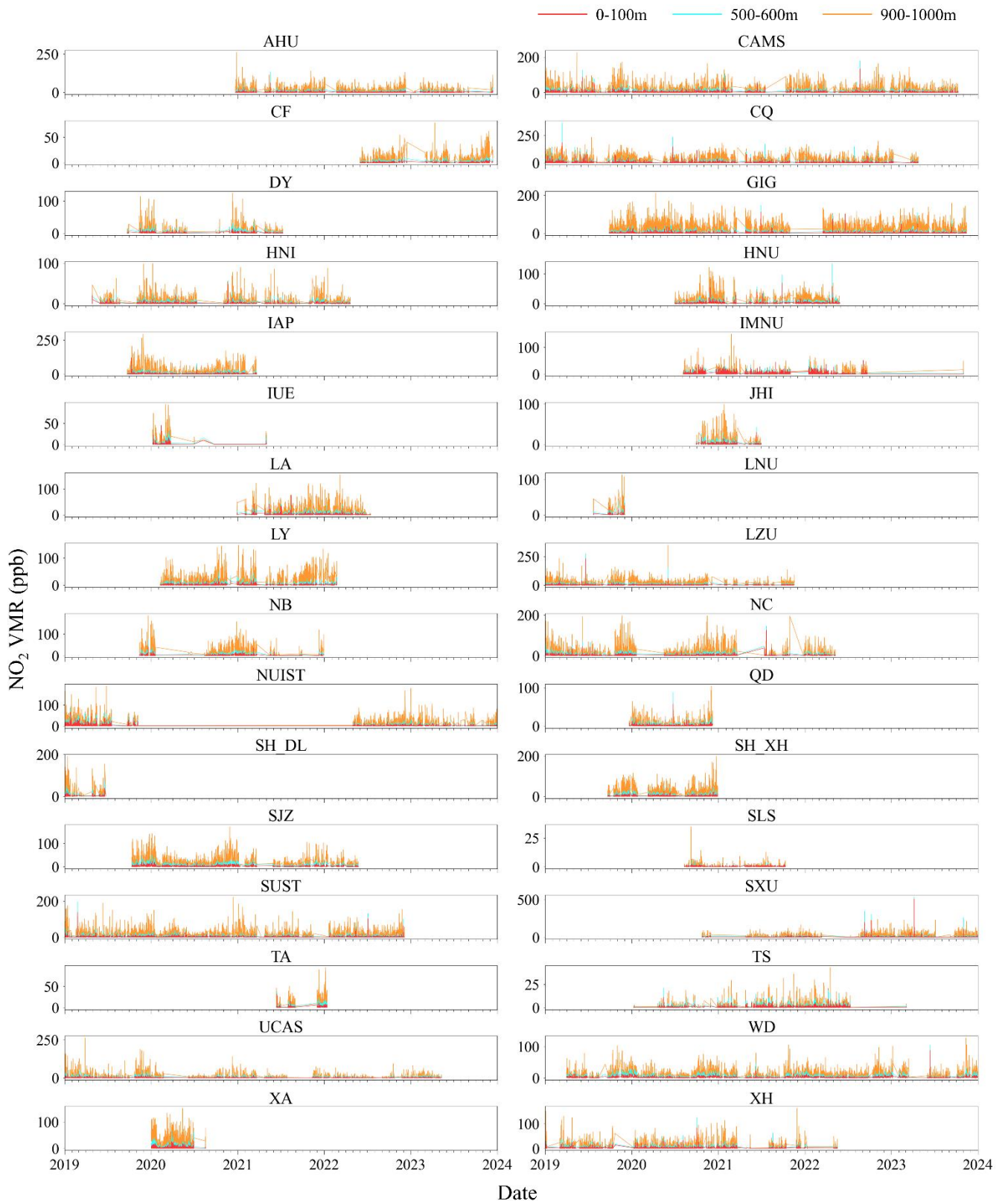
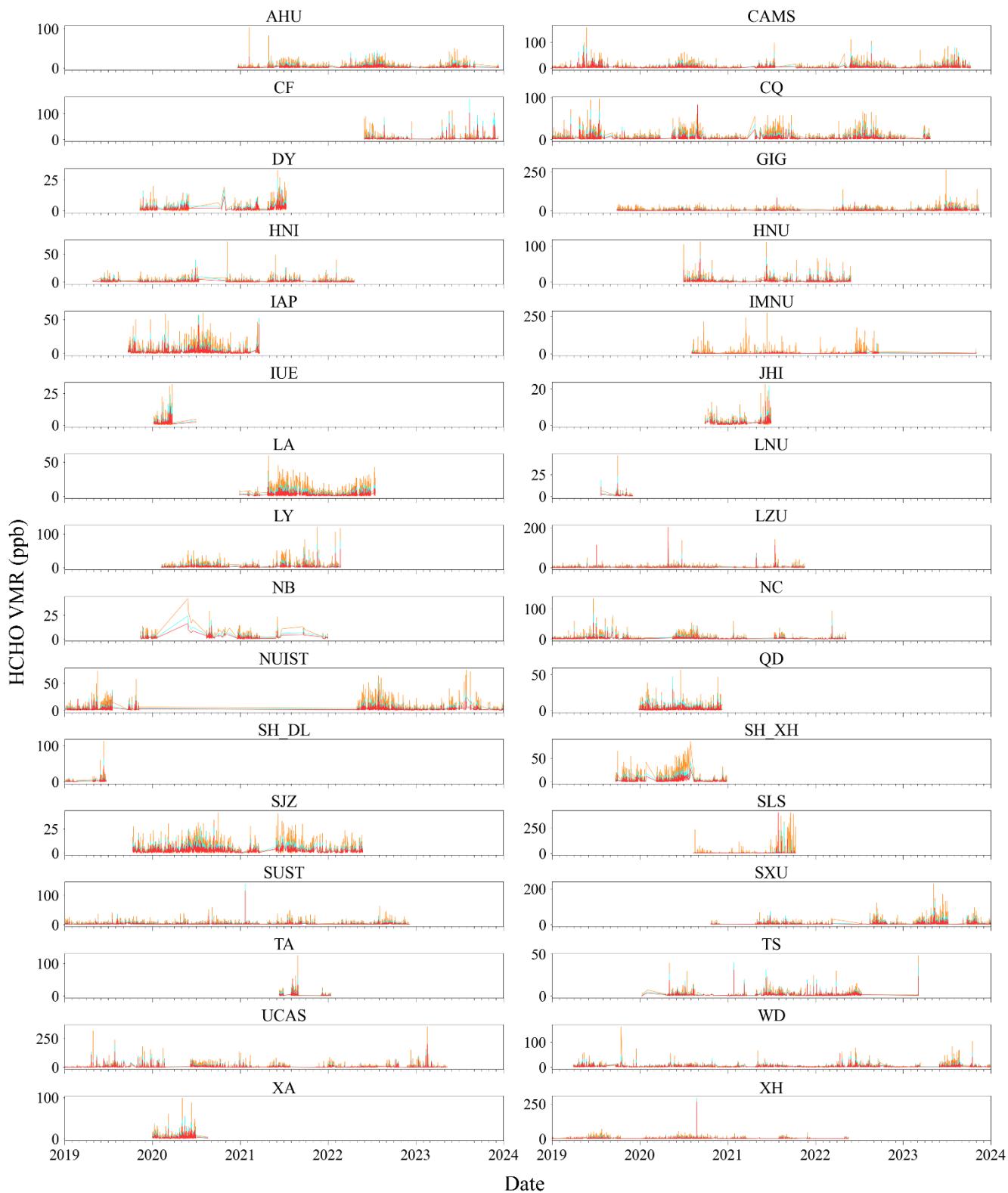


Figure S1. Time series of aerosol extinction during 2019-2023.



**Figure S2. Time series of NO<sub>2</sub> concentration during 2019-2023.**



**Figure S3. Time series of HCHO concentration during 2019-2023.**

3) Finally, discussion about the diurnal pattern of HCHO should be re-examined. For example, the evening peak of HCHO at the UCAS site was much enhanced than the IAP site (Figure 10), apparently, it could not be due to vehicular emissions during evening rush hours, as the former received much more traffic emissions (Figure 8).

Re: We sincerely appreciate your insightful comments, which have drawn our attention to this

phenomenon. The explanation for the observed evening peak of HCHO at the UCAS site is as follows: The UCAS site is located in a suburban area with relatively high vegetation coverage, leading to substantial emissions of volatile organic compounds (VOCs). Through photochemical reactions, VOCs contribute to the formation of HCHO, leading to its concentration accumulation over time (Nussbaumer et al., 2021). In the late afternoon (16:00–18:00), solar radiation weakens, leading to a reduction in HCHO photolysis and a decrease in its consumption rate (Biswas et al., 2020). Simultaneously, the lowering of the boundary layer height restricts pollutant dispersion, further contributing to the peak in HCHO concentration.

In response to your comment, we have revised the section discussing the diurnal pattern of HCHO. The updated content is as follows:

Line 321, “From 17:00 BJT, HCHO concentrations begin to rise again, peaking at 18:00 BJT, likely due to the lowering of the boundary layer (Franco et al., 2016). At certain suburban and rural sites, high vegetation coverage leads to substantial emissions of volatile organic compounds (VOCs) (Cao et al., 2022), which undergo photochemical reactions to produce HCHO, resulting in its accumulation over time (Nussbaumer et al., 2021). In the evening, the weakening of HCHO photolysis reduces its consumption, combined with the decrease in boundary layer height that limits dispersion, further enhances the concentration peak (Biswas et al., 2020).”

## List of other changes

“Table S1” -> “Table S4”

“Figure 2” -> “Figure 1”

“Figure 3” -> “Figure 2”

“Figure 4” -> “Figure 3”

“Figure 5” -> “Figure 4”

“Figure 6” -> “Figure 5”

“Figure 7” -> “Figure 6”

“Figure 8” -> “Figure 7”

“Figure 9” -> “Figure 8”

“Figure 10” -> “Figure 9”

“Figure 11” -> “Figure 10”

“Figure S1” -> “Figure S4”

“Figure S2” -> “Figure S5”

“Figure S3” -> “Figure S6”

“Figure S4” -> “Figure S7”

“Figure S5” -> “Figure S8”

“Figure S6” -> “Figure S9”

“Figure S7” -> “Figure S10”

“Figure S8” -> “Figure S11”

“Figure S9” -> “Figure S12”

“Figure S10” -> “Figure S13”

“Figure S11” -> “Figure S14”

“Figure S12” -> “Figure S15”

“Figure S13” -> “Figure S16”

“Figure S14” -> “Figure S17”

“Figure S15” -> “Figure S18”

“Figure S16” -> “Figure S19”  
“Figure S17” -> “Figure S20”  
“Figure S18” -> “Figure S21”  
“Figure S19” -> “Figure S22”  
“Figure S20” -> “Figure S23”  
“Figure S21” -> “Figure S24”  
“Figure S22” -> “Figure S25”  
“Figure S23” -> “Figure S26”  
“Figure S24” -> “Figure S27”  
“Figure S25” -> “Figure S28”  
“Figure S26” -> “Figure S29”  
“Figure S27” -> “Figure S30”  
“Figure S28” -> “Figure S31”

## Reference

- Biswas, M. S., Pandithurai, G., Aslam, M. Y., Patil, R. D., Anilkumar, V., Dudhambe, S. D., Lerot, C., De Smedt, I., Van Roozendaal, M., and Mahajan, A. S.: Effect of Boundary Layer Evolution on Nitrogen Dioxide (NO<sub>2</sub>) and Formaldehyde (HCHO) Concentrations at a High-altitude Observatory in Western India, *Aerosol Air Qual. Res.*, 21, 200193, <https://doi.org/10.4209/aaqr.2020.05.0193>, 2020.
- Buzcu Guven, B. and Olaguer, E. P.: Ambient formaldehyde source attribution in Houston during TexAQS II and TRAMP, *Atmospheric Environment*, 45, 4272–4280, <https://doi.org/10.1016/j.atmosenv.2011.04.079>, 2011.
- Cao, J., Situ, S., Hao, Y., Xie, S., and Li, L.: Enhanced summertime ozone and SOA from biogenic volatile organic compound (BVOC) emissions due to vegetation biomass variability during 1981–2018 in China, *Atmospheric Chemistry and Physics*, 22, 2351–2364, <https://doi.org/10.5194/acp-22-2351-2022>, 2022.
- Carlier, P., Hannachi, H., and Mouvier, G.: The chemistry of carbonyl compounds in the atmosphere—A review, *Atmospheric Environment (1967)*, 20, 2079–2099, [https://doi.org/10.1016/0004-6981\(86\)90304-5](https://doi.org/10.1016/0004-6981(86)90304-5), 1986.
- Franco, B., Marais, E. A., Bovy, B., Bader, W., Lejeune, B., Roland, G., Servais, C., and Mahieu, E.: Diurnal cycle and multi-decadal trend of formaldehyde in the remote atmosphere near 46° N, *Atmospheric Chemistry and Physics*, 16, 4171–4189, <https://doi.org/10.5194/acp-16-4171-2016>, 2016.
- Ho, S. S. H., Ho, K. F., Lee, S. C., Cheng, Y., Yu, J. Z., Lam, K. M., Feng, N. S. Y., and Huang, Y.: Carbonyl emissions from vehicular exhausts sources in Hong Kong, *Journal of the Air & Waste Management Association*, 62, 221–234, <https://doi.org/10.1080/10473289.2011.642952>, 2012.
- Jiao, P., Xing, C., and Liu, C.: A dataset of ground-based vertical profile observations of aerosol, NO<sub>2</sub> and HCHO from the hyperspectral vertical remote sensing network in China (2019-2023), <https://doi.org/10.5281/zenodo.14194965>, 2024.
- Lee, M., Heikes, B. G., Jacob, D. J., Sachse, G., and Anderson, B.: Hydrogen peroxide, organic hydroperoxide, and formaldehyde as primary pollutants from biomass burning, *Journal of Geophysical Research: Atmospheres*, 102, 1301–1309, <https://doi.org/10.1029/96JD01709>, 1997.
- Ma, Z., Liu, R., Liu, Y., and Bi, J.: Effects of air pollution control policies on PM<sub>2.5</sub> pollution improvement in China from 2005 to 2017: a satellite-based perspective, *Atmospheric Chemistry and Physics*, 19, 6861–6877, <https://doi.org/10.5194/acp-19-6861-2019>, 2019.
- Nussbaumer, C. M., Crowley, J. N., Schuladen, J., Williams, J., Hafermann, S., Reiffs, A., Axinte, R., Harder, H., Ernest, C., Novelli, A., Sala, K., Martinez, M., Mallik, C., Tomsche, L., Plass-Dülmer, C., Bohn, B., Lelieveld, J., and Fischer, H.: Measurement report: Photochemical production and loss rates of

formaldehyde and ozone across Europe, *Atmospheric Chemistry and Physics*, 21, 18413–18432, <https://doi.org/10.5194/acp-21-18413-2021>, 2021.

Ryan, R. G., Rhodes, S., Tully, M., Wilson, S., Jones, N., Frieß, U., and Schofield, R.: Daytime HONO, NO<sub>2</sub> and aerosol distributions from MAX-DOAS observations in Melbourne, *Atmospheric Chemistry and Physics*, 18, 13969–13985, <https://doi.org/10.5194/acp-18-13969-2018>, 2018.

Schauer, J. J., Kleeman, M. J., Cass, G. R., and Simoneit, B. R. T.: Measurement of Emissions from Air Pollution Sources. 5. C1–C32 Organic Compounds from Gasoline-Powered Motor Vehicles, *Environ. Sci. Technol.*, 36, 1169–1180, <https://doi.org/10.1021/es0108077>, 2002.

Song, Y., Xing, C., Liu, C., Lin, J., Wu, H., Liu, T., Lin, H., Zhang, C., Tan, W., Ji, X., Liu, H., and Li, Q.: Evaluation of transport processes over North China Plain and Yangtze River Delta using MAX-DOAS observations, *Atmospheric Chemistry and Physics*, 23, 1803–1824, <https://doi.org/10.5194/acp-23-1803-2023>, 2023.

Tan, W., Liu, C., Wang, S., Xing, C., Su, W., Zhang, C., Xia, C., Liu, H., Cai, Z., and Liu, J.: Tropospheric NO<sub>2</sub>, SO<sub>2</sub>, and HCHO over the East China Sea, using ship-based MAX-DOAS observations and comparison with OMI and OMPS satellite data, *Atmospheric Chemistry and Physics*, 18, 15387–15402, <https://doi.org/10.5194/acp-18-15387-2018>, 2018.

Wagner, T., Beirle, S., Remmers, J., Shaiganfar, R., and Wang, Y.: Absolute calibration of the colour index and O<sub>4</sub> absorption derived from Multi AXis (MAX-)DOAS measurements and their application to a standardised cloud classification algorithm, *Atmospheric Measurement Techniques*, 9, 4803–4823, <https://doi.org/10.5194/amt-9-4803-2016>, 2016.

Zheng, B., Tong, D., Li, M., Liu, F., Hong, C., Geng, G., Li, H., Li, X., Peng, L., Qi, J., Yan, L., Zhang, Y., Zhao, H., Zheng, Y., He, K., and Zhang, Q.: Trends in China's anthropogenic emissions since 2010 as the consequence of clean air actions, *Atmospheric Chemistry and Physics*, 18, 14095–14111, <https://doi.org/10.5194/acp-18-14095-2018>, 2018.